Comparison of Airborne and Terrestrial Gamma Spectrometry Measurements - Evaluation of Three Areas in Southern Sweden

Peder Kock
Christer Samuelsson

Department of Medical Radiation Physics, Clinical Sciences, Lund University
University Hospital, SE-221 85 Lund, Sweden

2011-05-18

Abstract

The Geological Survey of Sweden (SGU) has been conducting airborne gamma spectrometry measurements of natural radioactivity in Sweden for more than 40 years. Today, the database covers about 80% of the country's land surface. This article explores the first step of putting this data into use in radioactive source search at ground level. However, in order to be able to use the airborne background measurements at ground level, SGU data must be validated against terrestrial data. In this work, we compare the SGU data with data measured by a portable backpack system. This is done for three different areas in southern Sweden. The statistical analysis shows that a linear relationship and a positive correlation exist between the air and ground data. However, this linear relationship could be revealed only when the region possessed large enough variations in areal activity. Furthermore, the activity distributions measured show good agreement to those of SGU. We conclude that the SGU database could be used for terrestrial background assessment, given that a linear transfer function is established.

1 Introduction

When searching for radioactive sources using mobile in-situ gamma spectrometry, the background from naturally occurring radionuclides in the ground and in air (radon) can pose a challenge. Geology, topography, soil density and moisture as well as the detector itself are some of the parameters affecting the gamma radiation field. Apart from these inherent challenges the mobile gamma spectrometry platform is moving through the terrain, constantly sampling from a more or less unknown background. Research has been conducted in the field since the dawn of portable gamma spectrometers and numerous methods exist to separate the background from the sources of interest, in real-time (e.g. Cresswell and Sanderson, 2009; Hjerpe and Samuelsson, 2003; IAEA, 2003; Kock et al. 2010).

Airborne gamma spectrometry (AGS) is a swift and effective technique when broad geographic regions must be surveyed. Its applications include mineral exploration (Smith, 1985), geological mapping (Zhang et al., 1998), environmental assessment and assessment of uranium mine site rehabilitation (Bollhöfer et al., 2008; Martin et al., 2006), fallout mapping (Mellander, 1998) and radioactive source search (Cresswell and Sanderson, 2009; Ulvsand et al. 2003). If the survey area is small, ground based mobile gamma spectrometry can be a good alternative or complement to AGS. Having the detector close to the ground gives a much better spatial resolution. This field of view difference for the two techniques is also a factor that makes comparisons between the two less straight forward.

Most of the studies found in the literature, comparing measurements conducted by AGS to ground measurements, focus on either ^{137}Cs or dose rate comparisons, while comparisons made on the natural radiation background are rare. Comparisons between AGS and ground measurements in various forms are discussed in detail with respect to; soil sampling (Tyler et al. 1996), in-situ measurements (Bucher et al. 2000; Sanderson et al., 1995; Tyler et al., 1996) and kerma rates (Bargholz and Korsbech, 1997). International exercises including RESUME-95 and 99, RADMAGS and ECCOMAGS have also been undertaken in Europe, where ground to air comparisons, mainly for ^{137}Cs, are discussed and evaluated (Hoovgaard and Scott, 1997; Mellander et al. 2002; Sanderson et al. 2003, 2004).

Hoovgaard and Scott (1997) pointed out that a linear relationship between terrestrial and airborne measurements allows the possibility of scaling between the different sets. Sanderson et al. (2003) compared carborne ^{137}Cs measurements to airborne and found generally low R^2-values, with intercepts and scale factors significantly different from 0 and 1 respectively. However, they also compared ^{137}Cs activity and dose rates from in-situ measurements to AGS, which produced an excellent agreement between the two. Mellander et al. (2002) and Sanderson et al. (2003) found that the car-borne measurements underestimated activity with about 50% to those of AGS. This was explained by differences in the field of view and with the influence of roads.

Having a high quality background database opens up new possibilities in mo-

bile radioactive source search. Because of the (stochastic) natural background fluctuations and (systematic) environmental features it can be difficult to distinguish between a natural anomaly and an anthropogenic. Alarm algorithms tuned to detect anomalies typically suffer from so called type I (false positives) and type II (false negatives) errors (Barlow, 1989). *A priori* knowledge of the search area's activity distribution could, if properly incorporated in the alarm method, reduce the number of false alarms due to localised features and thus improve the search efficiency.

Airborne measurement campaigns measuring ^{40}K, ^{238}U and ^{232}Th have been carried out in Sweden since the late 1960's by the Geological Survey of Sweden (SGU). Today, SGU's database contains background data for about 80% of Sweden's area. Apart from its commercial and research applications, outlined above, this data cache offers potential *a priori* knowledge about the natural radiation background that could be used in mobile search operations at ground level, as recognized by IAEA (1990). However, before using the database in such a context it must be validated against terrestrial data. This article compares the AGS data to ground based measurements for three test areas in southern Sweden.

2 Survey sites

The Geological Survey of Sweden started their airborne gamma radiation measurements in the late 1960's, mainly to map uranium deposits. To this day SGU has potassium, uranium and thorium data for about 80% of Sweden, mainly excluding the mountain range along the Norwegian border. The grid consists of flight lines, flown during the snow-free season at 30-60 m altitude with 200-800 m line spacing. Data in the database are available as (radon stripped) concentrations along the flight lines. After the Chernobyl accident in 1986 SGU also mapped ^{137}Cs fallout (Mellander, 1988). However, radiocaesium will not be considered in this work.

Uranium (^{238}U) is measured through the radon daughter ^{214}Bi (1730+1765 keV, 18%) in its decay chain, while thorium (^{232}Th) is measured through ^{208}Tl (2614 keV, 99%) in its decay chain. Potassium (^{40}K) is measured directly at 1461 keV (11%). In geological surveys it is conventional to assume secular equilibrium in the decay chains of ^{238}U and ^{232}Th and report the results as equivalent uranium (eU) and equivalent thorium (eTh).

Three test areas were chosen for their different background compositions (Fig. 1). Table 1 summarise the basic characteristics and statistics for the three test areas. Apart from the different background levels between the areas, K, eU and eTh also vary significantly within some of the areas. An estimate of the area's variability is the Coefficient of Variation (CV), also given in Table 1.

Area I at Revingehed (N 55° 41.280', E 13° 30.350'), located 15 km east of Lund, was chosen for its homogeneous and low background levels. The geology consists of sedimentary rocks with a flat topography. Especially U and Th are unusually low here in a Swedish context (compare Table 1 to UNSCEAR (2000)).

	Area I			Area II			Area III			Unit
Area	1.02			0.54			0.42			km^2
Flight height	62.5			57.2			30			m
AGS samples	449			203			76			-
AGS samp. time	250			250			400			ms
Ground samples	2362			2325			1327			-
Ground samp. time	9			9			9			s
	Mean	SD	CV(%)	Mean	SD	CV(%)	Mean	SD	CV(%)	
AGS ^{40}K	446.5	124.3	27.9	504.9	228.6	45.3	722.5	252.4	34.9	Bq kg^{-1}
AGS eU	10.5	12.1	115.0	113.7	155.1	136.5	167.9	62.5	37.2	Bq kg^{-1}
AGS eTh	11.6	7.3	62.7	21.3	15.3	72.0	73.0	23.3	31.9	Bq kg^{-1}
Ground ^{40}K	3.19	0.98	30.7	5.12	1.90	36.9	5.81	2.29	39.5	counts s^{-1}
Ground eU	0.12	0.30	251.2	1.38	2.38	172.9	0.60	0.86	143.5	counts s^{-1}
Ground eTh	0.21	0.23	110.4	0.36	0.33	90.9	1.94	1.13	58.1	counts s^{-1}

Table 1: Summary characteristics and statistics for the three survey areas.

Any ground-to-air comparisons made for these both radionuclides within this area will suffer from bad statistics due to the low count rates.

Within area II, located at Andrarum (N 55° 43.017', E 13° 59.094') some 50 km east of Lund, the U-component varies strongly due to the presence of uranium-rich alun shale in the south-western part of the area. Area II also includes a small lake (Verkasjön) and some slag heaps from an old mine which further increases the background variation within the area. A small stream gorge (Verkan) crosses the area which is otherwise flat.

Area III is located west of Jämshög (N 56° 13.240', E 14° 27.068'), some 100 km north-east of Lund, where granite gneisses start to dominate the geology. The background radiation level is generally increased and locations with exposed rock and large boulders give raise to some fluctuations. The topography is mainly flat with the exception of a slope in the western part of the area.

3 Methodology

3.1 Statistical analysis

Rather than direct comparison of activities per unit mass, we compare the net counts from the terrestrial platform with the given concentrations from SGU. Both terrestrial and AGS survey data sets are gridded onto a 50x50 grid using a triangle-based linear interpolation algorithm; GRIDDATA, found in MATLAB[1]. The interpolation fits the data onto a non-smooth surface, thus the first derivative may have discontinuities.

The two surfaces (AGS and ground level) are then compared through their normalised distribution functions. This comparison shows the overall agreement of normalised data. Especially non-normal distributions are interesting, since it is an indication of localised high (compared to the surroundings) activity

[1]MATLAB is a software package produced and supported by The MathWorks, Inc, Natick, MA, USA.

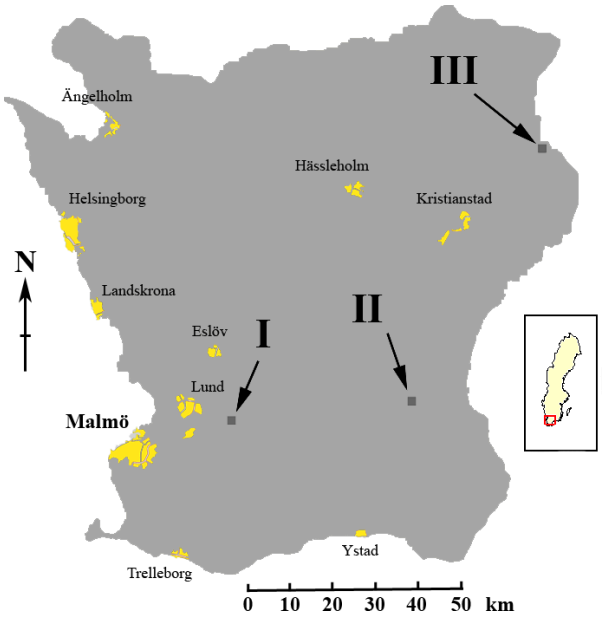

Figure 1: Map over Scania (Skåne), the southernmost region of Sweden. Major urban areas and the three survey areas (I-III) are marked on the map.

concentrations. However, studying the distribution functions does not give any information on the spatial correlation.

3.2 Linearity and spatial correlation

The linearity and spatial correlation are instead investigated in a scatter plot. As mentioned above, the field of view of the detectors differs significantly between the two data sets. The ratio between the areas covered by an airborne detector to the backpack detector is typically about 10^3 (Tyler et al., 1996). In order to account for the different field of views between the ground and air surveys a method to upscale the ground survey data is presented.

Instead of using the GRIDDATA interpolation, a circle is constructed around each AGS sample with a radius corresponding to 90% of the primary photon fluence, assuming a semi-infinite depth distribution and azimuthal symmetry. The fraction of the total primary photon fluence, $\phi_f(\theta, E)$, at a detector at height h above the ground plane is

$$\phi_f(\theta, E) = \frac{1}{E_2(\mu_a h)} \int_0^\theta \sin\varphi \;\; \exp(-\mu_a h \sec\varphi)\, d\varphi \tag{1}$$

where θ is the angle from the ground normal, h the height above ground, μ_a the

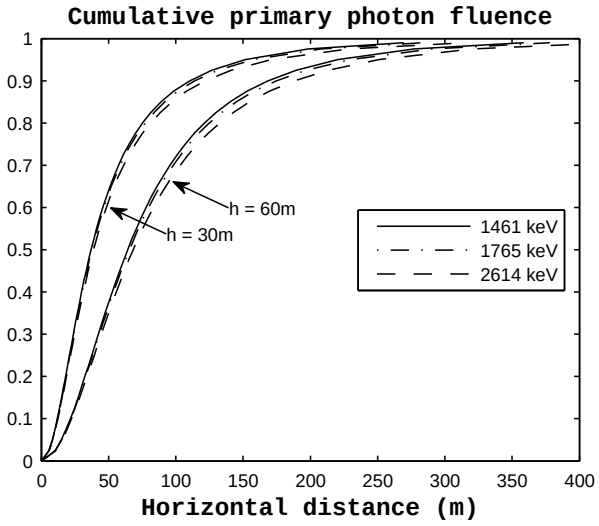

Figure 2: Cumulative primary photon fluence for a uniform depth distribution as a function of the horizontal distance (r). The two heights, 30m (three upper curves) and 60m (three lower curves), correspond to the mean flight heights used in the AGS surveys.

linear attenuation coefficient in air (Finck, 1992) and

$$E_2(x) = x \int_x^\infty t^{-2} \exp(-t)\, dt \tag{2}$$

is the second-order exponential integral. The 90% angle is obtained by solving for θ

$$\phi_f(\theta, E) = 0.9 \tag{3}$$

Now the 90% radius is simply

$$r = h \tan\theta \tag{4}$$

This procedure is repeated for $E = 1461, 1765$ and 2614 keV, thus obtaining three radii for each AGS sample. Fig. 2 shows solutions to the integral (1), presented as horizontal distances (Eq. (4)), for the three energies given above and the two typical AGS heights used in this work.

The results of the measurements conducted on ground within the calculated circle, u_i, are then summed together using inverse distance weighting

$$u(\mathbf{x}) = \sum_{i=0}^{n} \frac{w_i(\mathbf{x})}{\sum_{j=0}^{n} w_j(\mathbf{x})} u_i \tag{5}$$

where

$$w_i(\mathbf{x}) = \frac{1}{d(\mathbf{x}, \mathbf{x}_i)} \tag{6}$$

is the weighting function, $d(\mathbf{x}, \mathbf{x}_i)$ the distance between the AGS point, $\mathbf{x}$, and a sample point on the ground, $\mathbf{x}_i$ (Shepard, 1968).

3.3 Statistical Uncertainties

Unfortunately no measurement uncertainties are given in the SGU database. For the ground samples the uncertainty can be derived from the poisson standard deviations in the estimated net counts, i.e.

$$\sigma_i = \sqrt{N + B\Big(1 + \frac{n}{2m}\Big)} \tag{7}$$

where N is the net count, B the subtracted background count from m channels on either side of the region of interest, which is n channels wide (Gilmore, 2008). Assuming that no errors reside from the position acquisition, the weighted sample mean $u(\mathbf{x})$, defined in Eq. (5), has a standard deviation of

$$\sigma_u(\bar{x}) = 2\sqrt{\sum_{i=0}^{n} \omega_i^2 \sigma_i^2} \tag{8}$$

where

$$\omega_i = \frac{w_i(\mathbf{x})}{\sum_{j=0}^{n} w_j(\mathbf{x})} \tag{9}$$

is the total weight factor applied to sample i. Eq. (8) gives the total counting statistical uncertainty ($k = 2$) of the weighted sample mean, with a level of confidence of approximately 95%.

3.4 Data Sampling

The AGS surveys, shown in Fig. 3, contains data from lines flown at heights of about 60 m (area I and II) and 30 m (area III), with 200 m linespacing. Area I-II was surveyed in 1996, while the data from area III dates back to 1972. Measurement times were 250 ms for area I-II and 400 ms for area III. SGU data from before 1995 (i.e. area III) contains interpolated sample points with 40 m spacing along the flight line. Newer data (i.e. areas I-II) are recorded in the database at their sampling point. The AGS samples were smoothed along the flight lines, doubling the effective sample time to reduce the uncertainty from counting statistics. This was only necessary for the scatter plot analysis, were no interpolation was done on the SGU data set.

The terrestrial backpack survey was done in three stages during 2008-2010. Each area was surveyed during several hours of walking at pace of about 4-5 kmh^{-1}. A new spectrum was recorded to a laptop, which also was carried in

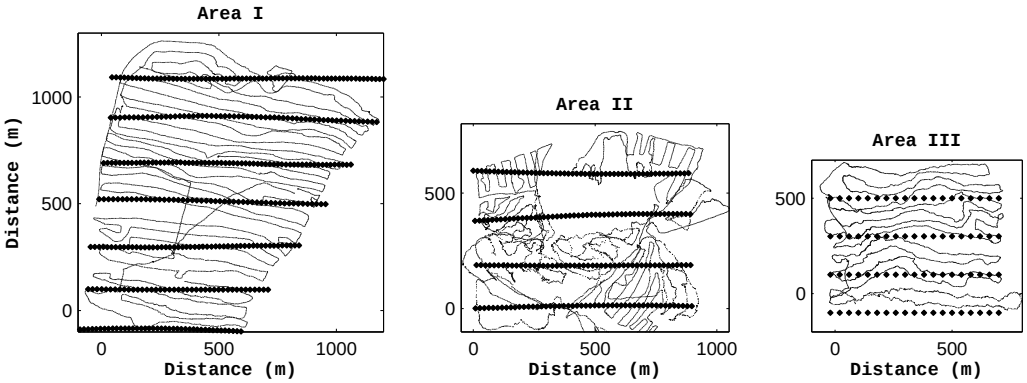

Figure 3: Plot of sample points for the three survey areas. Flight lines are seen as horizontal (east-western) bold markers while the ground surveys are plotted with small dots. Note the lake within area II, which can be seen indirectly as the area lacking terrestrial samples.

the backpack, every 3rd second, giving thousands of spectra. Along with each spectrum a GPS position was stored. The samples were then smoothed to give 9s samples, thus reducing the statistical counting uncertainty somewhat. Net counts from ^{40}K, ^{214}Bi and ^{208}Tl were evaluated using extended background regions on either side of the peak (Gilmore, 2008). The net count was stored along with two position elements, yielding three xyz data sets from each area.

4 Spectrometry Instrumentation

SGU uses a 16.7L NaI(Tl) mounted in a fixed-wing aircraft. The system was calibrated using four concrete pads, each with known concentrations of K, U and Th. The fourth pad is a null pad used for background correction. Unit spectra and stripping ratios were then calculated and used to measure terrestrial K, eU and eTh concentrations, assuming uniform depth distributions as described by the IAEA (IAEA 1991; ICRU 1994). At the time when area III was surveyed, SGU used a 6L NaI(Tl), calibrated by the same method. Both systems used an upward looking (currently 4L NaI(Tl)) detector to account for radon in the air.

The NaI(Tl) spectrometry system used in the ground survey is a portable backpack solution. It uses a 3x3" (7.62 x 7.62 cm) cylindrical detector from Saint-Gobain[2], model no. 3M3/3, equipped with a 14-pin photomultiplier tube, integrated bias supply, pre-amplifier and digital multi-channel analyser manufactured by Ortec (Ortec Digibase). The system was made for field use and

[2]Saint-Gobain Cristaux, 104 Route de Larchant, Nemours, France.

	Area I	Area II	Area III
K	0.98	0.95	0.96
eU	0.94	0.92	0.68
eTh	0.97	0.94	0.92

Table 2: Sample Pearson correlation coefficients between normalised airborne and normalised ground-based statistical distributions.

assembled by Gammadata[3].

The backpack was not calibrated for the geometry assumed in this work. Multiplying the net counts from the ground measurements with a calibration-constant does not give any additional information regarding the shape of the statistical distributions or the spatial correlation. Rather, a calibration and absolute comparisons would introduce an additional uncertainty to the comparison. Instead, all ground-to-air comparisons are made on normalised data.

5 Results and Discussion

5.1 Statistical distributions

The normalised distributions and cumulative distribution functions (cdf) of activity concentrations and net counts for SGU and backpack respectively are presented for K, eU and eTh in Figs. 4-6. Along with the survey samples a normal distribution fit is presented for comparison. Each bin has been normalised by the total number of samples, thus allowing for direct comparison of the two data sets within each subplot. Table 2 shows sample correlation coefficients (Pearson), r, between the AGS and ground data.

Potassium data in Fig 4, shows a very good agreement between the two surveys, for all three areas ($r \geq 0.95$). The distributions all have Gaussian shapes which gives no indication of local high activity concentration within any of the three areas. This can also be seen by studying the CV in Table 1, were both potassium rows show modest variability.

When studying the uranium graphs in Fig. 5, a few features immediately stand out, one being the non-Gaussian distribution of U-activity within area II. Still, the ground and air survey distributions showed a good agreement for this area ($r = 0.92$). Area I has a mean close to zero, which is due to the low U-levels within this area (see Table 1). Especially the ground survey suffers from poor statistics, mainly from the background subtraction, which can be seen in the relatively large proportion of the samples with negative values. Area III, however, which shows a much larger distribution width for the backpack, should not suffer from poor counting statistics. The distributions are both normal but the widths were far from equal ($r = 0.68$). This can partly be explained by interference from scattered ^{208}Tl 2614keV photons to the eU peak

[3]Gammadata Instrument AB, Vallong. 1, Uppsala, Sweden.

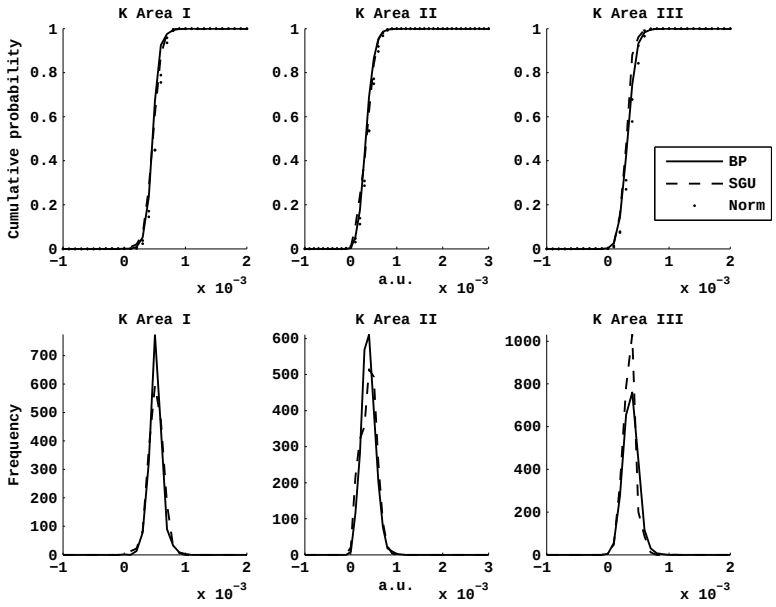

Figure 4: Normalised sample and cumulative distributions for ^{40}K, areas I-III. Two distributions are presented within each subplot, SGU's AGS (dashed lines) and backpack (BP, full lines). The top graphs also shows the cumulative distribution function of a fitted normal distribution.

(1765 keV). In fact, the backpack distribution fits the SGU data better when plotting gross counts, which is an indication of a failure in the background subtraction. Another possibility is that the higher variability of ground data is due to localised high activity concentrations which are smoothed in the AGS data[4].

Thorium data, shown in Fig. 6, also show a good agreement with $r \geq 0.9$. All three areas have gauss-like distributions, with slightly wider distributions for the terrestrial survey. Areas I and II have tails of negative values, again due to the relatively low mean activity concentration levels as shown in Table 1.

This analysis generally shows broader distribution peaks for the terrestrial surveys. One should bear in mind that the difference in field of view between the two detectors is not accounted for in this kind of analysis. Hence, the most important result from this analysis is that the general shapes of the distributions are the same. All but one (eU, area II) surveys are well described by a normal distribution, indicating one or many local high activity subareas within that area.

[4]As suggested by an anonymous reviewer.

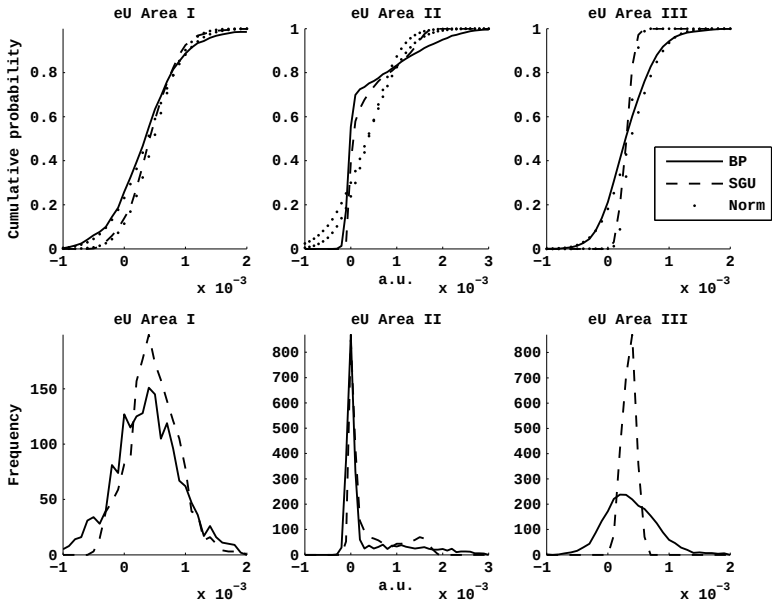

Figure 5: Normalised sample and cumulative distributions for eU, areas I-III. Two distributions are presented within each subplot, SGU's AGS (dashed lines) and backpack (BP, full lines). The top graphs also shows the cumulative distribution function of a fitted normal distribution.

5.2 Spatial correlation and linearity

5.2.1 Field of view

The smoothing technique outlined in the methodology section enables a direct comparison of ground and air measurements. However, the choice of primary fluence fraction, ϕ_f Eq. (3), needs to be explained. In theory, incorporating all measurements from the ground survey in every comparison, i.e. setting the radius r to be infinite, should yield a higher correlation, since all photons then are accounted for and properly weighted. In practice, however, this is not the case, as shown in Fig. 7. The coefficient of determination, R^2, was calculated for fractions of the total primary photon fluence in the range $0.7 \leq \phi_f \leq 0.99$. A value of less than 0.7 resulted in too few ground samples in some cases (especially for area III), why this was set as the lower bound. In Fig. 7 it can be seen that R^2 generally increases as the fraction of total photon increases to about 0.9. This is true for all data sets except eTh in area III, while $\phi_f > 0.9$ shows ambiguous results. The drop at larger values of ϕ_f can be explained by the finite extent of the ground survey. Samples close to the edges of the survey areas will be biased, especially if the radius is too large. As an example, consider an AGS sample in one of the corners of the survey area. The measurement will only have 25%

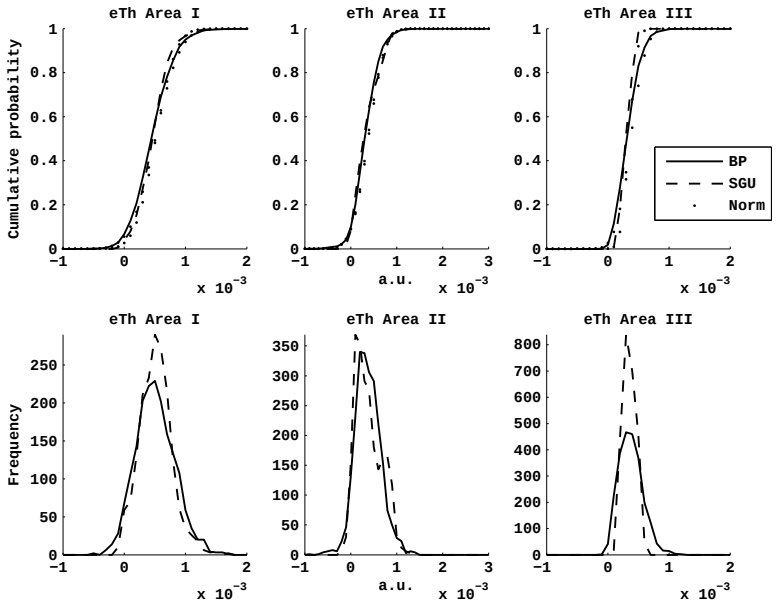

Figure 6: Normalised sample and cumulative distributions for eTh, areas I-III. Two distributions are presented within each subplot, SGU's AGS (dashed lines) and backpack (BP, full lines). The top graphs also shows the cumulative distribution function of a fitted normal distribution.

of its photons originating from the survey area, assuming homogeneous activity concentrations. The weighted ground sample will instead, at the same position, have all of its photons originating from the survey area. Therefore, setting the fraction to 0.9 seems to be a reasonable compromise.

5.2.2 Scatter plots

Fig. 8 shows scatter plots with AGS on the horizontal axis and weighted terrestrial data on the vertical axis. Ground data within the 90% radius (Eq. (4)) are weighted as defined in Eq. (5). Vertical uncertainties were then calculated according to Eq. (8). The result were normalised so that a good fit between AGS and terrestrial samples would lie on the straight line $y = x$.

The relative uncertainties of the weighted means, shown in Fig. 8, were generally in the order of a few to tens of percent, with a few exceptions. The uncertainty of each individual sample is greater, but when the samples are weighted and summed the uncertainty of the weighted sample mean drops. Generally, if there are n samples with equal weights and standard deviations, the standard deviation of the mean will decrease with a factor $1/\sqrt{n}$, according to the central limit theorem. Still some uranium samples incorporate the zero level within the given level of confidence (95%). Even though no uncertainties are given by

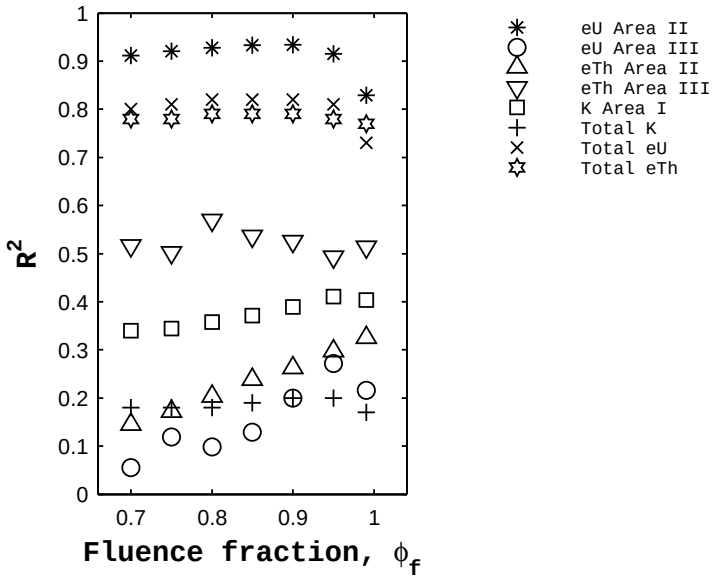

Figure 7: Coefficient of correlation, R^2, from the scatter plots of AGS and ground based samples, plotted against the fraction of total primary photon fluence. All comparisons, except eTh in area III, show greater R^2-values as the fraction is increased to 90% of the total primary photon fluence.

SGU, it is safe to assume that the uncertainties in the AGS samples are at least as great as the ones shown for the terrestrial samples. This is due to the number n, which is equal to one for all AGS samples.

Uranium in area II as well as thorium in area III show a good straight line fit between the two data sets. From the figure one can deduce that the mean and variability within the areas decide how good the straight line fit will be. Potassium, for instance, have a relatively small range of activities (which also can be seen in Fig. 4 and Table 1) within all three areas, yielding a poor correlation in the scatter plots.

To better understand the correlation between AGS and terrestrial data, Figs. 9-11 present scatter plots were all measurements from the three areas are presented together. Vertical errors are omitted, to make the figures more readable. Best straight line fits (least square), with 95% confidence intervals, and linear regression analyses R^2-statistic are also given in the figures. Again, the two background components with the largest variability (eU and eTh, Figs. 10-11) show strong positive correlations and good straight line fits, with slopes close to one and interceptions close to zero, while potassium (Fig. 9) shows a weak positive correlation.

The regression analysis is dominated by the area with the largest variability.

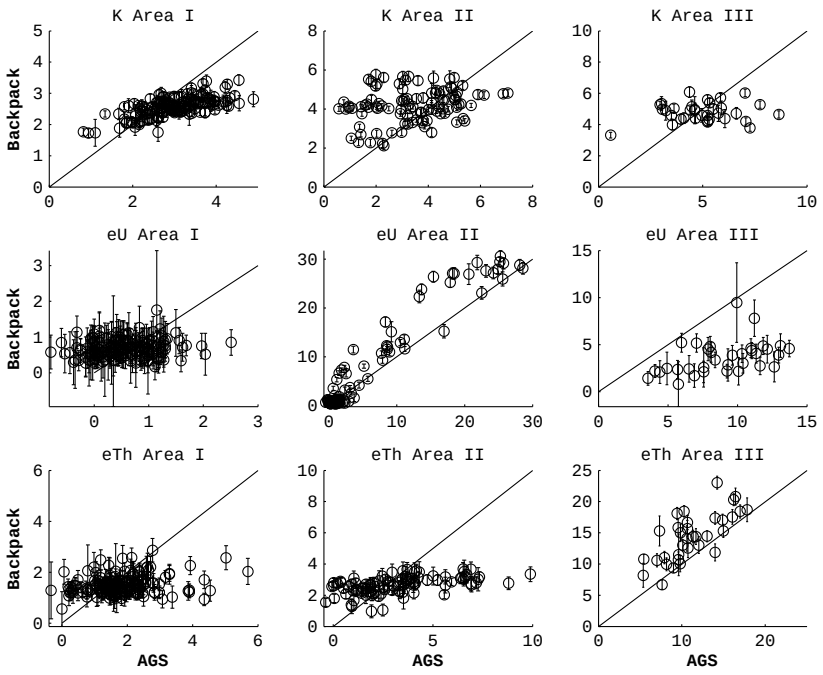

Figure 8: Scatter plots of ^{40}K, eU and eTh for areas I-III. Normalised backpack count rates (vertical) with uncertainties ($k = 2$) versus normalised AGS concentrations (horizontal). Solid lines, $x = y$, are given in each subplot. Note the relatively large uncertainties in samples from area I compared to areas II-III.

In both Fig. 10 and Fig. 11 two clusters with different slopes can be seen. Uranium data from area III exhibit a much smaller slope than eU data from area II, while eTh data from area II exhibit a much smaller slope than eTh data from area III. In both figures the area with the most activity lies above the regression line. Most likely this is an effect due to the field of view difference, discussed above. The sensitivity to local variations are higher in the ground measurements, which reflects in clusters on either side of the $x = y$ line. It is also possible that airborne activity contribute to the ground based measurements, as no radon stripping was done in the terrestrial measurements. The results suggest that the ground data upscaling model presented in this work might fail for a single area, but that it gives satisfactory results if enough variability can be found in the data.

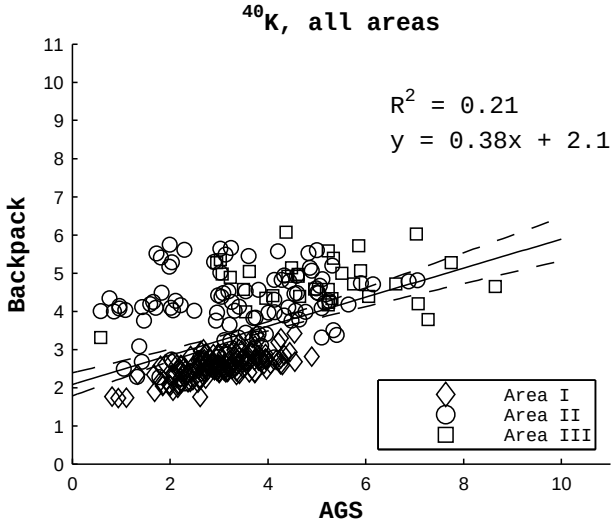

Figure 9: Scatter plot of normalised ^{40}K samples. Dashed lines show 95% confidence interval for regression line. A weak positive correlation exists, with non-zero intercept and a slope significantly different from unity.

6 Conclusions

This study presents a model for upscaling of ground data to compensate for the field of view difference between AGS and ground data. Using the model we show that spatial ground-to-air correlation analysis on normalised data is feasible. Regression analysis of eU and eTh gave slopes close to one and intercepts close to zero, while ^{40}K only showed a weak positive correlation with slope and intercept significantly different from one and zero, respectively. The results show that the spatial correlation between AGS and ground data is stronger in areas where the activity variability is large; given a large enough mean activity. These areas also tend to be the most challenging in ground based mobile radioactive source search operations. The strong spatial correlation between AGS and ground data for eU and eTh suggests that a linear transfer function can be established.

We have also shown that comparisons directly between air and ground spectral data can be made using the normalised distributions of the whole area. All but one distribution were normal, while eU in area II contained localised high radiation areas and thus a non-Gaussian distribution. Such non-Gaussian areas are especially problematic when searching for radioactive sources. They could trigger a false alarm of type I, when moving into, or type II, when moving out of, the area in question. Having a distribution shape from AGS data could therefore be part of a prognostic tool, to be used when conducting terrestrial radioactive search operations.

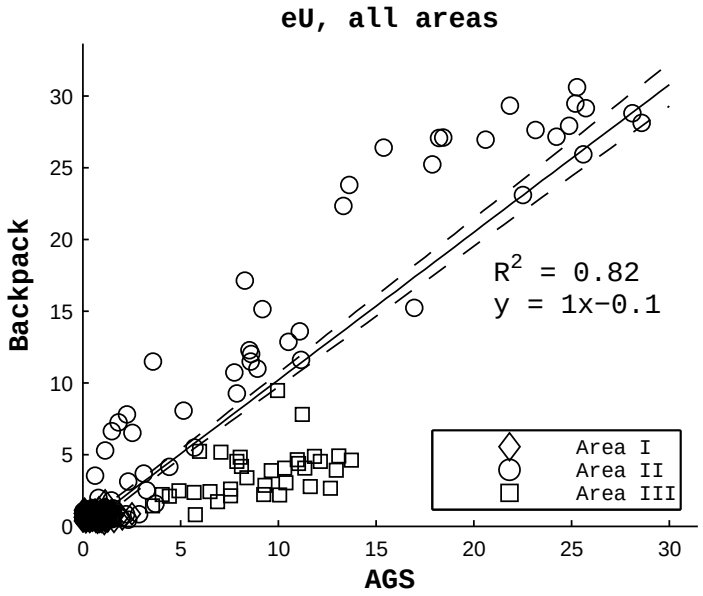

Figure 10: Scatter plot of normalised eU samples. Dashed lines show 95% confidence interval for regression line. The regression gives unity slope and intercept close to zero, which shows a good agreement between ground and air measurements for eU.

Acknowledgements

The authors wish to thank Sören Byström, Mats Wedmark and Johan Daniels at SGU for their feedback and help with making the SGU database available to us. Thanks also to Jonas Nilsson, Lund University, for his insightful suggestions. This work was supported by the Swedish Radiation Safety Authority, SSM.

References

[1] Bargholz, K., Korsbech, U., 1997. Conversion of airborne gamma ray spectra to ground level air kerma rates, in: Bäverstam, U., Fraser, G., Kelly, G.N. (Eds.), Decision making support for off-site emergency management, Proceedings of fourth international workshop, Aronsborg, Sweden, October 7-11 1996. Radiat. Prot. Dosimetry 73(1-4), pp. 127-130. Nuclear Technology Publishing, Ashford, UK. ISBN 1-87096-549-3.

[2] Barlow, R.J., 1989. Statistics: a guide to the use of statistical methods in the physical sciences. John Wiley & Sons Ltd., New York.

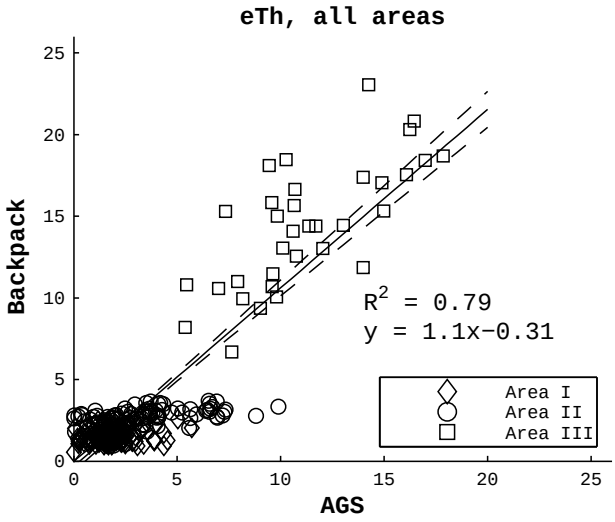

Figure 11: Scatter plot of normalised eTh samples. Dashed lines show 95% confidence interval for regression line. A strong positive correlation exist, the straight line has an intercept and slope close to zero and unity respectively.

[3] Bollhöfer, A., Pfitzner, K., Ryan, B., Martin, P., Fawcett, M., Jones, D.R., 2008. Airborne gamma survey of the historic Sleisbeck mine area in the Northern Territory, Australia, and its use for site rehabilitation planning. J. Environ. Radioact. 99, 1770-1774.

[4] Bucher, B., Rybach, L., Schwarz, G., 2000. Environmental mapping: comparison of ground and airborne spectrometry results under alpine conditions, in: Sanderson, D.C.W., McLeod, J.J. (Eds.), Recent applications and developments in mobile and airborne gamma spectrometry. Proceedings of the RADMAGS symposium, University of Stirling, 15-18 June 1998, SURRC, University of Glasgow.

[5] Cresswell, A.J., Sanderson, D.C.W., 2009. The use of difference spectra with a filtered rolling average background in mobile gamma spectrometry measurements. Nucl. Instr. Methods Phys. Res. A 607, 685-694.

[6] Finck, R. R., 1992. Doctoral Dissertation. High resolution field gamma spectrometry and its applications to problems in environmental radiology. Departments of radiation physics, Malmö and Lund, Lund University. pp. 1-138. Kristianstads boktryckeri, Malmö, Sweden. ISBN: 91-628-0739-0.

[7] Gilmore, G., 2008. Practical gamma-ray spectrometry, 2nd Edition. Wiley-VCH Verlag, Weinheim.

[8] Hjerpe, T., Samuelsson, C., 2003. A comparison between gross and net count methods when searching for orphan radioactive sources. Health Phys. 84(2), 203-211.

[9] Hoovgard, J., Scott, E.M., 1997. RESUME-95: Results of an international field test of mobile equipment for emergency response, in: Bäverstam, U., Fraser, G., Kelly, G.N., Decision making support for off-site emergency management. Proceedings of fourth international workshop, Aronsborg, Sweden, October 7-11 1996. Radiat. Prot. Dosimetry 73(1-4), pp. 219-224. Nuclear Technology Publishing, Ashford, UK. ISBN 1-87096-549-3.

[10] International Atomic Energy Agency (IAEA), 1990. The use of gamma ray data to define the natural environment. IAEA-TECDOC-566. Vienna, Austria.

[11] International Atomic Energy Agency (IAEA), 1991. Airborne gamma ray spectrometer surveying. Technical Report Series 323. Vienna, Austria.

[12] International Atomic Energy Agency (IAEA), 2003. Guidelines for radioelement mapping using gamma ray spectrometry data. IAEA-TECDOC-1363. Vienna, Austria.

[13] International Commission on Radiation Units and Measurments (ICRU), 1994. Gamma-ray spectrometry in the environment. ICRU Report 53. Maryland, USA.

[14] Kock, P., Finck, R.R., Nilsson, J.M.C., Östlund, K., Samuelsson, C., 2010. A deviation display method for visualising data in mobile gamma-ray spectrometry. Appl. Radiat. Isot. 68, 1832-1838.

[15] Martin, P., Timis, S., Mcgill, A., Ryan, B., Pfitzner, K., 2006. Use of airborne γ-ray spectrometry for environmental assessment of the rehabilitated Nabarlek uranium mine, Australia. Environ. Monit. Assess. 116, 531-553.

[16] Mellander H., 1998. Airborne gammaspectrometric measurements of the fall-out over Sweden after the nuclear reactor accident in Chernobyl, USSR. Swedish Geological Co, Report TFRAP 8803. Uppsala, Sweden.

[17] Mellander H., Aage H.K., Karlsson S., Korsbech U., Lauritzen B., Smethurst M., 2002. Mobile gamma spectrometry. Evaluation of the Resume 99 exercise. NKS-56. NKS, Roskilde. ISBN 87-7893-111-8.

[18] Sanderson, D.C.W., Allyson, J.D., Tyler, A.N., Scott, E.M., 1995. Environmental applications of airborne gamma spectrometry, in: IAEA Technical Committee Meeting on the use of uranium exploration data and techniques in environmental studies. Proceedings of a technical committee meeting. Vienna, Austria 9-12 November 1993, IAEA-TECDOC-827, pp. 71-92. Vienna, Austria.

[19] Sanderson, D.C.W., Cresswell, A.J., Scott, E.M., Lauritzen, B., Karlsson, S., Strobl, C., Karlberg, O., Lang, J.J., 2003. Report on exercise data comparisons, in: An international comparison of airborne and ground based gamma ray spectrometry. University of Glasgow, 2003, pp. 9-174. ISBN: 0-85261-783-6.

[20] Sanderson, D.C.W., Cresswell, A.J., Scott, E.M., Lang, J.J., 2004. Demonstrating the European capability for airborne gamma spectrometry: results from the ECCOMAGS exercise. Radiat. Prot. Dos. 109, 119-125.

[21] Shepard, D., 1968. A two-dimensional interpolating function for irregularly-spaced data. Proceedings of the 1968 23rd ACM national conference, pp. 517-524.

[22] Smith, R.J., 1985. Geophysics in Australian mineral exploration. Geophysics, 50(12), 2637-2665.

[23] Tyler, A.N., Sanderson, D.C.W., Scott, E.M., Allyson, J.D., 1996. Accounting for spatial variability and fields of view in environmental gamma ray spectrometry. J. Environ. Radioact. 33, 213-235.

[24] Ulvsand, T., Finck, R.R., Lauritzen, B. (Eds) 2003. NKS/SRV seminar on Barents Rescue 2001 LIVEX gamma search cell. NKS-54. NKS, Roskilde. ISBN: 87-7893-108-8.

[25] UNSCEAR, 2000. Sources and effects of ionizing radiation, volume 1: sources. United Nations scientific committee on the effects of atomic radiation, report to the general assembly, United Nations, New York.

[26] Zhang, Y., Xiong, S., Chen, T., 1998. Application of airborne gamma-ray spectrometry to geoscience in China. Appl. Radiat. Isot. 49, 139-146.